THE ASTROPHYSICAL JOURNAL, 637:L93–L96, 2006 February 1

CONSTRAINED COSMOLOGICAL SIMULATIONS OF DARK MATTER HALOS

EMILIO ROMANO-DIAZ,[1,2] ANDREAS FALTENBACHER,[3] DANIEL JONES,[2,4] CLAYTON HELLER,[4]
YEHUDA HOFFMAN,[1] AND ISAAC SHLOSMAN[2]

Received 2005 August 10; accepted 2005 December 22; published 2006 January 19

ABSTRACT

The formation and structure of dark matter halos are investigated by means of constrained realizations of Gaussian fields using *N*-body simulations. Experiments in the formation of a $10^{12}\ h^{-1}\ M_{\odot}$ halo are designed to study the dependence of the density profile on its merging history. We find that (1) the halo growth consists of several violent and quiescent phases, with the density well approximated by the Navarro-Frenk-White (NFW) profile at most times; (2) the NFW scale radius R_s stays constant during the quiet phases and grows abruptly during the violent ones, while the virial radius grows linearly during the quiet phases and grows abruptly during the violent phases; (3) the value of R_s reflects the violent merging history of the halo; (4) the central density stays unchanged during the quiet phases while dropping abruptly during the violent ones (its value does not reflect the formation time of the halo); and (5) the clear separation of the evolution of an individual halo into series of quiescent and violent phases explains the inability to fit its entire evolution by simple scaling relations, in agreement with previous studies.

Subject headings: dark matter — galaxies: evolution — galaxies: formation — galaxies: halos — galaxies: interactions — galaxies: kinematics and dynamics

Online material: color figures

1. INTRODUCTION

The issue of the formation and structure of dark matter halos constitutes one of the outstanding challenges of modern cosmogony. It is easily formulated as what is the outcome of the collapse and virialization of bound perturbations in an otherwise homogeneous and isotropic expanding universe. This is further simplified by considering only collisionless noninteracting particles, i.e., dark matter (DM). The resulting collapsed objects are dubbed here as *halos*. This seemingly lucid problem does not easily yield itself to an analytical understanding and is addressed here in a series of numerical "experiments."

Studies of the collapse and virialization of structures in an expanding universe date to the early times of modern cosmogony. The only exact analytical solution relevant to the problem is that of a single spherical density perturbation in a Friedmann universe—the secondary infall model (Gunn 1977; Fillmore & Goldreich 1984; Bertschinger 1985; Hoffman & Shaham 1985; Ryden & Gunn 1987; Zaroubi & Hoffman 1993). The shortcomings of this analytical approach prompted the study of the formation of DM halos by means of *N*-body simulations (e.g., White 1976). The structure of DM halos inferred from the cosmological models and power spectra of the primordial perturbation field was found to be well approximated by a spherically averaged density profile (Navarro et al. 1996, hereafter NFW),

$$\rho(r) = \frac{4\rho_s}{(r/R_s)(1 + r/R_s)^2}, \tag{1}$$

where ρ_s is the density at the scale radius R_s. The NFW profile constitutes a universal fit to the structure of DM halos over many orders of magnitudes in mass and at different redshifts. It has been confirmed by numerous *N*-body simulations, although some authors indicate that the inner slope might be steeper (e.g., Moore et al. 1998; Fukushige & Makino 2001) or shallower (Subramanian et al. 2000; Taylor & Navarro 2001; Ricotti 2003) than NFW, or that it depends on the halo mass (Jing & Suto 2000). The origin of the NFW profile has been studied in the framework of the secondary infall model (e.g., Nusser & Sheth 1999; Lokas & Hoffman 2000; Nusser 2001; Ascasibar et al. 2004) and the merger scenario (Syer & White 1998; El-Zant 2005). Analytical models necessarily invoke spherical symmetry or a very simplified merging picture, but no theory has been suggested that accounts for the emergence of the NFW (or its variants) profile in the wide range of cosmological models and settings that numerical simulations exhibit. This has led us to embark on a series of numerical experiments carefully designed to shed light on the problem.

It has been determined by Wechsler et al. (2002, hereafter W02), Zentner & Bullock (2003), Zhao et al. (2003a, 2003b; hereafter collectively Z03), and Salvador-Solé et al. (2005) that the evolution of DM halos proceeds in two phases of rapid and slow accretion. The general understanding that has followed is that an NFW structure is quickly established after the rapid phase and is preserved during the slow accretion. Hence, the emergence and/or evolution of the NFW profile might depend primarily on the merger's epoch (e.g., Syer & White 1998; El-Zant 2005; Dehnen 2005). We design a set of numerical experiments in which a halo of $10^{12}\ h^{-1}\ M_{\odot}$ (h is the Hubble constant in units of 100 km s^{-1} Mpc^{-1}) is constrained to follow *different merging histories.* Such controlled experiments can only be performed by constrained simulations—any differences in the final structure should be attributed to this process. A major virtue of constrained simulations is their ability to impose specific constraints in order to manipulate and allow a fine-tuned study of DM halo growth. This provides an additional insight into the details of violent phases in the halo evolution dominated by mergers.

A major effort was aimed at studying the evolution of the NFW parameters of an ensemble of halos (e.g., W02; Z03;

[1] Racah Institute of Physics, Hebrew University, Jerusalem 91904, Israel.
[2] Department of Physics and Astronomy, University of Kentucky, Lexington, KY 40506-0055.
[3] Physics Department, University of California, Santa Cruz, CA 95064.
[4] Department of Physics, Georgia Southern University, P.O. Box 8031, Statesboro, GA 30460.

Salvador-Solé et al. 2005; Reed et al. 2005) by fitting simple scaling relations to the NFW parameters. The resulting scatter around these relations was found to be considerable. We test whether this scatter is intrinsic, due to the NFW fitting procedures, or whether it follows from the fact that individual halos do not obey these relations. Our approach is based on the ability to design the initial conditions for *N*-body simulations by constrained realizations of Gaussian fields (Hoffman & Ribak 1991; see also van de Weygaert & Bertschinger 1996).

2. CONSTRAINED SIMULATIONS AND MODELS

We used the updated FTM-4.4 hybrid code (Heller & Shlosman 1994; Heller 1995), with $N \sim 2.1 \times 10^6$. The forces are computed using the routine falcON (Dehnen 2002), which is about 10 times faster than the optimally coded Barnes & Hut (1986) tree code. The gravitational softening is $\epsilon = 500$ pc. To follow the collapse of an individual halo in an expanding Friedmann universe, we used vacuum boundary conditions and physical coordinates. In these coordinates, the cosmological constant, Λ, or its generalization as dark energy appears explicitly in the acceleration equation but is not included in the FTM. Therefore, we assumed the open cold dark matter (OCDM) model with $\Omega_0 = 0.3$, $h = 0.7$, and $\sigma_8 = 0.9$ (where Ω_0 is the current cosmological matter density parameter and σ_8 is the variance of the density field convolved with a top-hat window of radius 8 h^{-1} Mpc used to normalize the power spectrum). This is very close to the "concordance" ΛCDM model in dynamical properties. We follow the dynamical evolution of the density profile and its dependence on the merging history, and therefore the results obtained here are also valid in a ΛCDM cosmology. The code was tested in the cosmological context using the Santa Barbara Cluster model (Frenk et al. 1999).

A series of linear constraints on the initial density field are used to design the numerical experiments. All the constraints are of the same form, namely, the value of the initial density field at different locations, and evaluated with different Gaussian smoothing kernels, with their width fixed so as to encompass a mass M (the mass scale on which a constraint is imposed). The set of mass scales and the location at which the constraints are imposed define the numerical experiment. Assuming a cosmological model and power spectrum of the primordial perturbation field, a random realization of the field is constructed from which a constrained realization is generated using the Hoffman & Ribak (1991) algorithm.

A set of five different models, i.e., experiments, is designed here to probe different merging histories of a given $10^{12}\ h^{-1}\ M_\odot$ halo in an OCDM cosmology. This halo is constrained to have different substructures on various mass scales and locations designed to collapse at different times according to the spherical top-hat model. This serves as a rough guide as the substructures are neither spherical nor isolated. Furthermore, the few constraints used here do not fully control the experiments. The nonlinear dynamics can, in principle, affect the evolution in a way not fully anticipated from the initial conditions. Even more important is the role of the random component of the constrained realizations (Hoffman & Ribak 1991). Thus, depending on the nature of the constraints and the power spectrum assumed, the random part can provide significant substructures at different locations and mass scales. This can be handled by adding more constraints and varying their numerical values.

Model A (our benchmark model) is based on two constraints. One is that of a $10^{12}\ h^{-1}\ M_\odot$ halo at the origin designed to collapse at $z_c = 2.1$. This halo is embedded in a region (second constraint) with $10^{13}\ h^{-1}\ M_\odot$ where the overdensity is zero, corresponding to an unperturbed Friedmann model. This scale is larger by a factor of 3 (in mass) than the computational sphere. Therefore, the constraint cannot be fulfilled exactly, yet it constrains the large-scale modes of the realizations to be zero. These two constraints are imposed on all models. Model B adds two substructures of $5 \times 10^{11}\ h^{-1}\ M_\odot$ within the $10^{12}\ h^{-1}\ M_\odot$ halo ($z_c = 3.7$). Model C further splits model B halos into two $2.5 \times 10^{11}\ h^{-1}\ M_\odot$ substructures ($z_c = 5.7$). Thus, the benchmark halo is designed to follow two major mergers to virialize. Model D uses model A and imposes six different small substructures of $10^{11}\ h^{-1}\ M_\odot$ ($z_c = 7.0$) scattered within the large halo. Model E simulates a more monolithic collapse in which a nested set of constraints, located at the origin, is set on a range of mass scales down to $M = 10^{10}\ h^{-1}\ M_\odot$ ($z_c = 6.9$). All models have been constructed with the same seed of the random field. All the density constraints constitute 2.5–3.5 σ perturbations (where σ^2 is the variance of the appropriately smoothed field) and were imposed on a 128^3 grid of $L = 4\ h^{-1}$ Mpc. The shortcoming of the present simulations is that we miss part of the external torque that should act on the final $10^{12}\ h^{-1}\ M_\odot$ halo. Yet, this affects only the final phase of the formation of the halo. At earlier times, the main halo is surrounded by others of about the same mass, which dominate the torque. The linear initial density fields are evolved numerically from $z = 120$ to $z = 0$, and their evolution was sampled with 165 time outputs spaced logarithmically in the expansion parameter a. Each halo is resolved at $z = 0$ with $\sim 1.2 \times 10^6$ particles within $R_{\rm vir}$.

3. RESULTS

All models differ substantially at early epochs, with a subsequent convergence in some of their properties but not in others. They lead to the formation of a single object of $\sim 10^{12}\ h^{-1}\ M_\odot$ via mergers with the surrounding substructure and via a slow accretion. To analyze the clumpy substructure, we define a DM halo as having the mean density equal to some critical value Δ_c times the critical density of the universe, where Δ_c depends on z and the cosmological model. The top-hat model is used to calculate $\Delta_c(z)$, and the density is calculated within a virial radius ($R_{\rm vir}$). The halos are identified initially by the HOP algorithm (Eisenstein & Hut 1998) and approximated by means of a radius $R_{\rm vir}$. Comparison of the HOP halos with those of the standard friends-of-friends halo finder (Davis et al. 1985) shows good agreement. Given a group catalog, a merger tree is constructed using all the snapshots.

The evolution toward the final halo is studied by tracking back in time the main branch leading to this halo. The general picture that emerges is that of a halo undergoing phases of *slow* and ordered evolution *intermitted* by episodes of rapid mass growth *via* collapse and *major mergers* (e.g., W02; Z03). These are referred to as the quiescent and violent phases.

The structure of a halo is studied by fitting it to an NFW profile (eq. [1]) and following the cosmological evolution of the NFW parameters, namely, R_s and $R_{\rm vir}$. Other fits (Moore et al. 1998; Jing & Suto 2000; and a generalized NFW fitting) have been attempted—our results and trends reported here appear independent of the fitting procedure. The fitting algorithm used is based on logarithmic binning of the halo into spherical shells, and estimating R_s by minimal χ^2, where the residual in a given shell is normalized by its own density. The fitting is performed within $\min(0.6R_{\rm vir}, 0.5d_H)$, where d_H is the distance

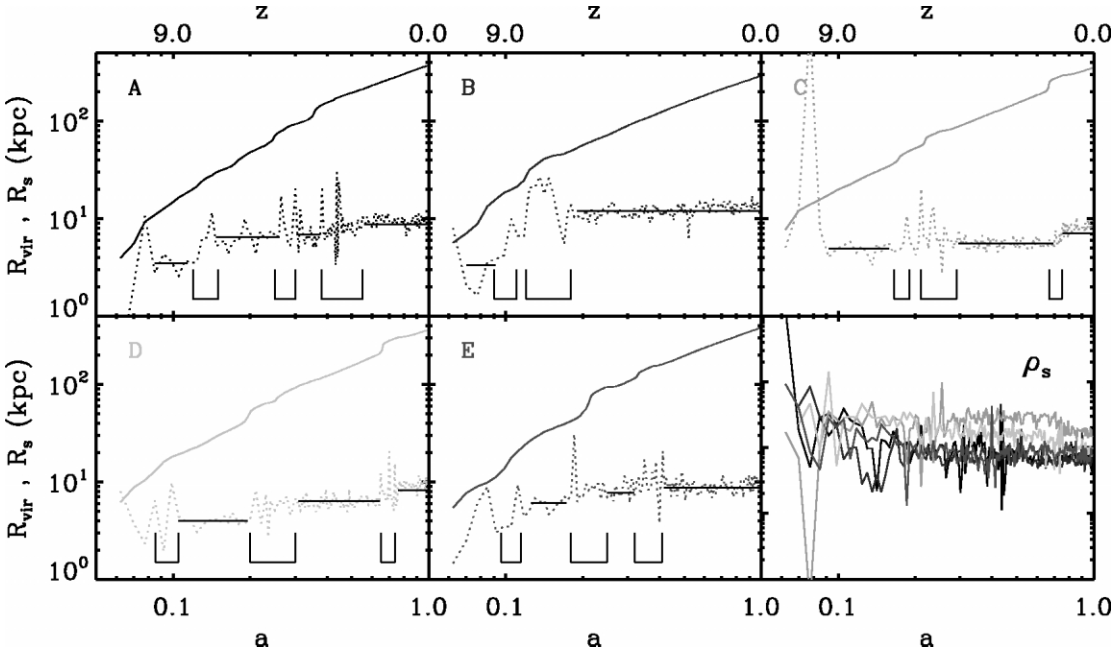

FIG. 1.—Behavior of virial and scale radii (*solid and dotted lines, respectively*) as a function of a for models A, B, C, D, and E. The discontinuous growths in R_s and R_{vir} match the violent phases that each halo passes through. The horizontal bars represent the mean value of R_s within the quiescent phases. The square brackets delineate the length of the violent phases. The bottom right panel shows the evolution of ρ_s (in arbitrary units), with the colors corresponding to the models in the other panels. [*See the electronic edition of the Journal for a color version of this figure.*]

to the nearest massive halo. Although the spherical symmetry of an NFW model ignores some of the dynamical properties of a halo, we use it as the first approximation to the halo structure. The NFW profile is found to constitute a very good fit to the spherically symmetric density in the quiescent phases, in agreement with numerous other studies. During the violent phases, such as mergers of nearly equal mass halos or the collapse of a few substructures to form a single halo, the halos are out of equilibrium and do not follow the NFW profile (e.g., Syer & White 1998).

The evolution of R_s and R_{vir} of the main halo for all the models is presented in Figure 1. The R_{vir} (accretion) trajectories show a regular behavior and a linear growth (W02), separated by abrupt increases associated with the violent phases. Most strikingly, R_s remains *constant* in the quiescent phases and grows *discontinuously* in the violent ones—subject to an ~5%–10% jitter in the quiescent phases that grows stronger during the violent phases when the halos get out of a dynamical equilibrium. The horizontal bars represent R_s averages in the quiescent phases. The bottom brackets indicate the duration of the mergers, computed by looking at variations that are >20% in R_s between contiguous output times.

The scale density ρ_s shows the opposite behavior—remaining constant in the quiescent phases and decreasing abruptly in the violent ones, except model C for which ρ_s increases slightly during a quiet phase. We note that all models, except B, converge to the same value of R_s (within the jitter) at $a \sim 0.8$–1, in spite of the different tracks leading to it. In model B, the two major halos have already turned around but have yet to merge. Even before this last merger, R_s is larger than in the other models and is expected to grow further.

The present simulations show that there is no simple relation between ρ_s and the timing of the violent phases. The order of models given by their last violent phase is B, E, A, D, and C. Yet, all the models have similar ρ_s except for model C, which has a value twice as large (Fig. 1). Note that one can define the halo formation time as the epoch at which the halo mass is half its final value (e.g., NFW; W02) or as the time of the last violent phase. In either case, we find that the central density cannot be used as an indicator of the formation time.

The dynamical evolution of the main halos has been analyzed in terms of the internal kinetic energy (K) within R_s and R_{vir}. Any perturbation in the halo's internal state (violent mass aggregation, random energy acquisition, etc.) will be reflected in its K_s behavior. We find that K_s behaves similarly to R_s—remaining constant during the quiescent stages (within the jitter) and growing discontinuously during the violent phases. This implies a possible correlation between K_s and R_s, which has been tested by measuring the relative changes of K_s vs. R_s—Figure 2 confirms this behavior. The changes in K_s and R_s are computed by averaging these quantities over the quiescent phases and taking differences between the consecutive ones (E. Romano-Diaz et al. 2006, in preparation). The internal kinetic energy computed within R_{vir} shows a similar behavior but grows very slowly during the quiescent phases.

4. DISCUSSION

The halo growth can be divided into the violent and quiescent phases analyzed in our superior time-sampled N-body simulations using constrained realizations. This allowed us to perform a detailed study of the evolution of a given halo under a variety of merging histories. This Letter focuses on the evolution of R_s and R_{vir}. The main new results are as follows: (1) The NFW scale R_s stays constant during the quiescent phases and changes abruptly during the violent ones. In contrast, R_{vir} grows linearly in the quiescent phases and abruptly during the violent phases; (2) ρ_s stays unchanged during the quiescent phases and drops abruptly during the violent ones. (3) The value of R_s reflects the violent merging history of the halo and depends on the number of violent events and their fractional magnitudes, independent of their time and order. As a corollary, ρ_s does not reflect the formation time

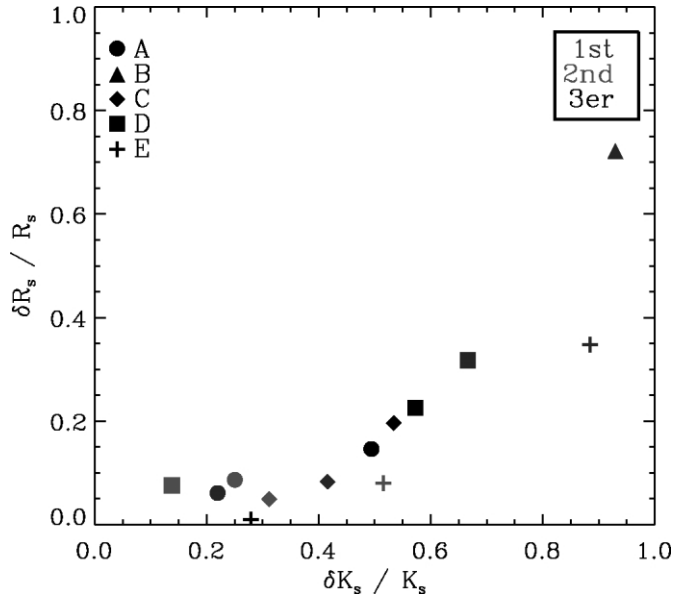

FIG. 2.—Fractional variations in the internal kinetic energy within R_s, $\delta K_s/K_s$, vs. those in the scaling radius, $\delta R_s/R_s$, before and after the violent phases. The colors correspond to different generations of major mergers. [*See the electronic edition of the Journal for a color version of this figure.*]

of the halo. (4) The fractional change in R_s is a nonlinear function of the fractional absorbed kinetic energy within R_s in a violent event. (5) The fact that the evolution of a given halo consists of a few quiescent phases intermitted by violent episodes implies that simple scaling relations can be applied to a single accretion trajectory but cannot be used to bridge and extend over a few such trajectories. This explains the scatter found in the accretion trajectories of single halos around fitted scaling relations, yet some of it can be attributed to the inadequacy of the analytical density profiles (see also Reed et al. 2005). We note that the accretion trajectories in all models converge to the same value—a reflection of the large-scale structure shared by all the models and imposed by the constrained initial conditions.

The advantage of the constrained realizations lies in its unique ability to generate a series of models with one or more parameters varied in a controlled fashion, while all others are held fixed. It enables us to cleanly separate the cause-and-effect relationship between the initial parameters and the outcome of the dynamical evolution. This complements the prevailing method of large-scale cosmological simulations in which issues of structure and evolution are addressed statistically. The scaling relations found in such a statistical analysis are not necessarily applicable to an individual halo. Here we focus on the role of the merging history in the halo evolution, by imposing density constraints based on the top-hat model. Our method provides us with the opportunity to test objectively the role of the merging history in shaping the structure of DM halos. The analogy between thermodynamical processes involving entropy and the dynamics of halos as manifested by the evolution of the scale radius R_s has not escaped our attention. We shall elaborate on this issue elsewhere.

The results obtained in this Letter pertain to a single halo in the framework of an OCDM cosmology. Yet, the conclusions reached from our set of experiments are relevant to the understanding of halo formation in CDM cosmologies in general and ΛCDM cosmology in particular.

We acknowledge fruitful discussions with A. Klypin. This work was supported by ISF-143/02 and the Sheinborn Foundation (Y. H.), by NSF/AST 00-98351 and NASA/NAG5-13275 (A. F.), by NASA/LTSA5-13063, NASA/ATP NAG5-10823, and HST/AR-10284 (I. S.), and by NSF/AST 02-06251 (C. H., I. S.). E. R.-D. was supported by the Golda Meier fellowship at the HU.

REFERENCES

Ascasibar, Y., Yepes, G., Gottlöber, S., & Müller, V. 2004, MNRAS, 352, 1109
Barnes, J., & Hut, P. 1986, Nature, 324, 446
Bertschinger, E. 1985, ApJS, 58, 39
Davis, M., Efstathiou, G., Frenk, C. S., & White, S. D. M. 1985, ApJ, 292, 371
Dehnen, W. 2002, J. Comput. Phys., 179, 27
———. 2005, MNRAS, 360, 892
Eisenstein, D. J., & Hut P., 1998, ApJ, 498, 137
El-Zant, A. A. 2005, MNRAS, submitted (astro-ph/0502472)
Fillmore, J. A., & Goldreich, P., 1984, ApJ, 281, 1
Frenk, C. S., et al. 1999, ApJ, 525, 554
Fukushige, T., & Makino, J. 2001, ApJ, 557, 533
Gunn, J. E. 1977, ApJ, 218, 592
Heller, C. H. 1995, ApJ, 455, 252
Heller, C. H., & Shlosman, I. 1994, ApJ, 424, 84
Hoffman, Y., & Ribak, E. 1991, ApJ, 380, L5
Hoffman, Y., & Shaham, J. 1985, ApJ, 297, 16
Jing, Y. P., & Suto, Y. 2000, ApJ, 529, L69
Lokas, E., & Hoffman, Y. 2000, ApJ, 542, L139
Moore, B., Governato, F., Quinn, T., Stadel, J., & Lake, G. 1998, ApJ, 499, L5
Navarro, J. F., Frenk, C. S., & White, S. D. M. 1996, ApJ, 462, 563 (NFW)
Nusser, A. 2001, MNRAS, 325, 1397
Nusser, A., & Sheth, R. K. 1999, MNRAS, 303, 685
Reed, D., Governato, F., Quinn, T., Gardner, J., Stadel, J., & Lake, G. 2005, MNRAS, 359, 1537
Ricotti, M. 2003, MNRAS, 344, 1237
Ryden, B. S., & Gunn, J. E. 1987, ApJ, 318, 15
Salvador-Solé, E., Manrique, A., & Solanes, J. M. 2005, MNRAS, 358, 901
Subramanian, K., Cen, R., & Ostriker, J. P. 2000, ApJ, 538, 528
Syer, D., White, S. D. M. 1998, MNRAS, 293, 337
Taylor, J. E., & Navarro, J. F. 2001, ApJ, 563, 483
van de Weygaert, R., & Bertschinger, E. 1996, MNRAS, 281, 84
Wechsler, R. H., Bullock, J. S., Primack, J. R., Kravtsov, A. V., & Dekel, A. 2002, ApJ, 568, 52 (W02)
White, S. D. M. 1976, MNRAS, 177, 717
Zaroubi, S., & Hoffman, Y. 1993, ApJ, 416, 410
Zentner, A. R., & Bullock, J. S. 2003, ApJ, 598, 49
Zhao, D. H., Jing, Y. P., Mo, H. J., & Börner, G. 2003a, ApJ, 597, L9
Zhao, D. H., Mo, H. J., Jing, Y. P., & Börner, G. 2003b, MNRAS, 339, 12